Micromechanical alternatives to phenomenological hardening plasticity

By: Itai Einav* and Giang D. Nguyen
School of Civil Engineering, The University of Sydney, Sydney, NSW 2006, Australia
*Corresponding author; email: i.einav@civil.usyd.edu.au

Abstract

Phenomenology is often applied in science through curve-fitting experimental results. This can be quite a useful exercise as long as it is not possible to derive a theory that can describe the observed results using first principles. Some of the most classical models of soil mechanics are in fact heavily based on curve-fitting procedures. Such models – e.g., critical state soil mechanics and kinematic hardening plasticity – are kept being used albeit the possibility to derive laws that are based on first principles. This may be fine if the mathematical structure of the alternative models is more difficult to apply. Here, however, we demonstrate that this is not always the case. It is possible to derive model alternatives to critical state soil mechanics and kinematic hardening plasticity that are based on first principles and that are equivalently mathematically simple.

1. Introduction

Phenomenological curve-fitting can be very useful when it is not possible to derive a theory that can explain the observed results using first principles. However, curve-fitting is strictly limited to describing only the set of observable experiments. It is then possible to combine the curve-fitting equations with a mathematical framework, in order to predict conditions beyond the experiments. The mathematical framework of plasticity is a convenient way for such an extension for the modelling of materials, which is a popular procedure in the soil mechanics community (both in academia and practice).

While the use of curve-fitting models is still the predominant tool of characterisation in practice, soil mechanics research is gradually learning to accept the role of first principles; this is evident through the increasing popularity of the discrete element method (Cundall and Strack, 1979), i.e., using Newton's laws of motion. Yet it is hard to predict *when* and *if* the use of the discrete simulations could ever be adequate for engineering practice. '*When*' is the question of computer power, which is a particularly relevant when large-scale engineering problems are at stake. The question of '*if*' arises because the discrete element method does not fully resolve the need for constitutive assumptions: instead of using models of representative volume element, here the problem converts into defining particle contact models. Phenomenology then quickly finds its way back, although with less support from experiments that at the micro scale turn to be more complex.

The derivation of effective and simple constitutive models, based on first principles, provides a good reconciliation between the practical requirement for convenient solutions to large-scale problems and the academic pursuit of fundamental understanding. However, deriving effective constitutive models that are both simple and that are based on first principles is easier said than done. As a result, some of the most classical models of soil mechanics are in fact rooted on curve-fitting procedures; often those are structured mathematically using the theory of plasticity. Such models – e.g., critical state soil mechanics and kinematic hardening plasticity – are kept being used for their simplicity and ability to explain some of the observed behaviour, but not necessarily for adequate use of first-principles. Here, we present alternative theories for the kinematic hardening plasticity and critical state models, which are equally simple and that are based on clear first-principles of statistical homogenisation and energy balance.

Mathematical models of non-hardening plasticity involve the definition of a single stationary yield surface in stress-space. Within the yield surface the constitutive behaviour is kept elastic, while the onset of yielding manifests inelastic deformations, accompanied by energy dissipation. These models are mathematically convenient, but geomaterials present a much more complicated

behaviour. Stress-strain investigations using elementary material tests reveal the following trends: (1) in cyclic shear tests hysteresis behaviour is observed, and (2) the yield threshold is ever increasing under continuously increasing isotropic pressure. To *implicitly* recover these aspects, traditional constitutive modelling of geomaterials involves, respectively: (1) multi-surface kinematic hardening, and (2) isotropic hardening (as in critical state soil mechanics).

The purpose of this paper is to motivate simple micromechanics explanations to the roots of these phenomena. We present alternative modelling concepts that *explicitly* adopt the micromechanical roots of both the isotropic and kinematic hardening phenomena. The two alternative formulations are equally simple, can describe the same phenomenological aspects *explicitly* rather than *implicitly*, and provide additional information that relates to meaningful microscopically-based variables and physical parameters.

2. Kinematic hardening plasticity and micromechanical roots

2.1. Phenomenological analog model

Consider the observable curve shown in Fig. 1 representing the stress-strain response of an elementary material to a given conceptual mechanical experiment. This example is certainly not new, but it serves an easy entrance into our discussion. In the spirit of phenomenological plasticity let us look at the material as a black box, without questioning what it is actually made of. As we load the material we see a linear stress-strain response, characterised by a slope E, which we call the elastic Young's modulus. However, as we keep loading the material beyond a certain stress threshold, σ_u, we observe a change to the slope from E to K. Upon unloading and reloading, the stress threshold seems to 'kinematically' change its value. In order for the abrupt change in slope, 'yield', to occur in the unloading direction, an opposite increment of stress is needed that equals $2\sigma_u$. We call this effect 'kinematic hardening', and 'feel ready' to propose a phenomenological constitutive model.

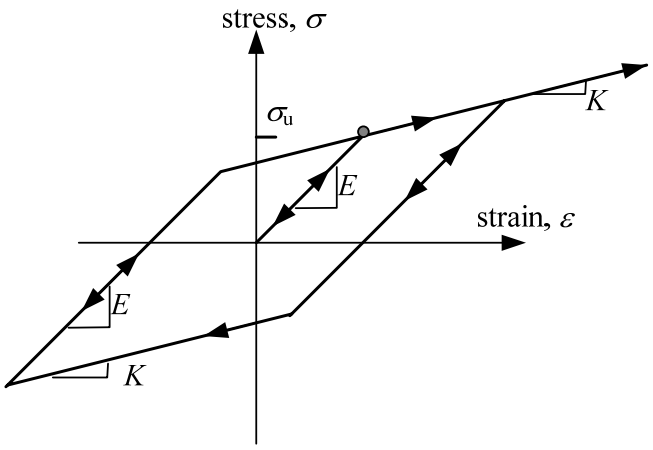

Figure 1. stress-strain curve observed as an outcome of a conceptual mechanical experiment

It is well-known that data of Fig. 1 could be replicated in exact manner by a 1D mechanical analog of a spring with a stiffness modulus H placed in parallel with a slider with stress threshold

$$k = \sigma_u \,, \tag{1}$$

both of which are placed in a series with another spring of modulus E (see Fig. 2).

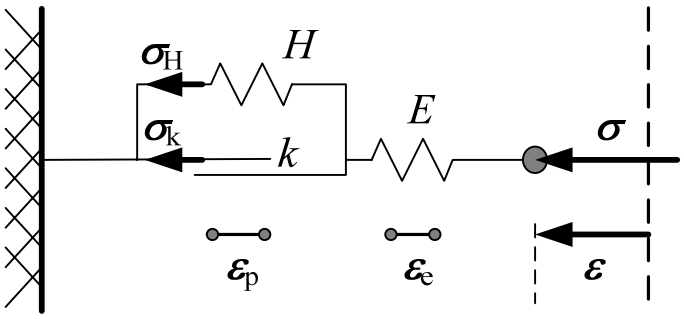

Figure 2. mechanical analog that is capable of curve fitting the result shown in Fig. 1.

From geometrical compatibility and force/stress equilibrium it follows that:

$$\varepsilon = \varepsilon_e + \varepsilon_p \;;\quad \sigma = \sigma_H + \sigma_k \tag{2}$$

where $\varepsilon_e = \sigma / E$ and $\varepsilon_p = \sigma_H / H$ are the elastic deflection/strain within the springs E and H; ε_p is also the macroscopic plastic strain, signifying the overall permanent deformation; σ and ε are the force/stress and the deflection/strain acting externally to the entire mechanical analog; σ_k, the force/stress within the slider, must always satisfy the 'yield criterion':

$$y = {\sigma_k}^2 - k^2 = \left(\sigma - H\varepsilon_p\right)^2 - k^2 \le 0 \tag{3}$$

Considering eqs. (2) and (3) for the yield situation (y=0), we write $\varepsilon = \sigma / E + (\sigma - k) / H$ (assuming that the element is loaded in the positive direction). Therefore during yield the tangential slope K in Fig.1 could be captured by setting H to satisfy:

$$K = \frac{EH}{E + H} \tag{4}$$

One can safely conclude that the model above does not violate the fundamental laws of mechanics since it is reproduced directly from a physically-based mechanical analog. It can even be shown that it satisfies the first and second laws of thermodynamics (Maugin, 1992). However, note that the 'real' material is not made out of two springs and a single slider. The analog (or use of thermodynamics) is merely giving us the convenient framework for a consistent mathematical derivation. It tells us nothing about the micromechanics and what the actual material is made of. If microscopic information is not available, then the model is as good as any other model. However, if microscopic information becomes available, we should question whether it is possible to assign physical meaning to the analog's structure and properties.

2.2. Alternative analog model

An alternative 1D analog model defines the mechanical system of two parallel springs, E_i ($i = a, b$; see Fig. 3a), each of which is placed in a series with a corresponding sliding element of threshold k_i ($i = a, b$). Following the logic in the previous section it can be shown that by assigning particular values to the parameters it is possible to deduce exactly the stress-strain curve shown in Fig. 1. For example, we start by requiring that

$$E = E_a + E_b, \tag{5}$$

This condition enables to predict the initial elastic slope in Fig. 1. Equilibrium further suggests that

$$\sigma = \sigma_a + \sigma_b \tag{6}$$

where σ_i ($i = a, b$) is the local stress in either one of the two analog's legs. Again, the slider must satisfy the 'yield criterion':

$$y_i = {\sigma_i}^2 - {k_i}^2 \le 0 \;\; (i = a, b) \tag{7}$$

Compatibility requires that $\varepsilon_a = \varepsilon_b = \varepsilon$, with $\varepsilon_i = \varepsilon_{e,i} + \varepsilon_{p,i}$. The local stresses are given by the elastic law of the individual springs, $\sigma_i = E_i \varepsilon_{e,i}$, therefore the yield surfaces can be represented in total strain space using $y_i = \left(E_i(\varepsilon - \varepsilon_{p,i})\right)^2 - k_i^2 \le 0$ $(i = a, b)$. If we further require that one of the slider threshold would never be reached, e.g., say $k_b \to \infty$, then because $\sigma_b = E_b \varepsilon$ ($\varepsilon_{p,b}$=0) and using the equilibrium eq. (6) we confirm that upon yielding ($\sigma_a = k_b$) the tangential stress-strain slope is $\partial\sigma / \partial\varepsilon = E_b$. Therefore, using eq. (5) we can set the stiffness parameters to fit the observed slopes:

$$E_b = H\,; \quad E_a = E - H \tag{8}$$

For the case of $k_b \to \infty$ first yielding (in the other slider) occurs when $\varepsilon_{p,a} = 0$, in which case $(E - H)\varepsilon = k_a$ ($\varepsilon_{e,b} = \varepsilon$). Therefore, by demanding that the analog provides first yielding according to the observed experiment, $\sigma = \sigma_u$, and noting the equilibrium eq. (6), we use

$$k_a = \frac{E - H}{E}\sigma_u\,, \tag{9}$$

This shows that the stress-strain curve in Fig. 1 can be replicated by the current analog, exactly as the previous analog managed to do.

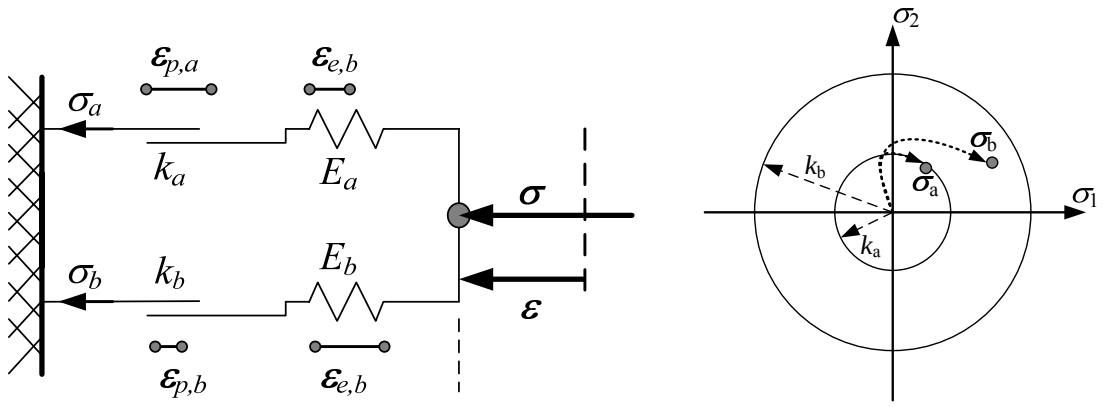

(a) (b)

Figure 3. (a) a second mechanical analog. This analog is also capable of replicating the results in Fig. 1. However, this time it is possible to assign physical meaning to the analog's parameters, as we demonstrate in section 2.3. (b) the extension of the model to account for the more general stress model is possible by replacing the 1D sliders using yield surface (here via a 2D representation).

In the next section we will show that this time (unlike the previous analog) it is possible to assign physical meaning to the analog's parameters. Before we continue to do that, it is useful to note the generalisation of this analog to the more general situation of stress tensors. This is made possible simply by replacing the local stress scalars in the yield equations (7), by local stress tensors:

$$y_i = 2\boldsymbol{\sigma}'_i : \boldsymbol{\sigma}'_i - k_i^2 \le 0 \;\; (i = a, b) \tag{10}$$

where the bold notation denotes a tensor (e.g., $\boldsymbol{\sigma}_i$ would be the stress tensor in element i); $\boldsymbol{\sigma}'_i$ is the deviatoric part of $\boldsymbol{\sigma}_i$; the symbol ':' designates dot product between the tensors. The generalisation requires a constitutive evolution equation for the local plastic strain tensors. Thermodynamics is then becoming handy, showing (Einav and Collins, 2008) that the local plastic strain incremental change is then given by the local flow rule:

$$\delta\boldsymbol{\varepsilon}'_{p,i} = \lambda_i \partial y_i / \partial \boldsymbol{\sigma}'_i = 2\lambda_i \boldsymbol{\sigma}'_i \;\; (i = a, b) \tag{11}$$

For more complete detail on the thermomechanical aspect of this model we recommended the paper by Einav and Collins (2008). At this point, however, what we have shown is sufficient to demonstrate that the extension of the second analog to general stress condition means that the local 1D sliders could now be described by yield surfaces (see Fig 3b for a 2D representation), whose flow rule are associated according to eq. (11). Unlike conventional models of kinematic hardening plasticity, here the yield surfaces are inert in space of unit element forces (here, the forces along the analog's legs) and the hysteresis effects are captured by gradual yielding thanks to the variable nature of the local stresses.

2.3. The micromechanical interpretation of the second analog

We have just managed to demonstrate that from a phenomenological point of view there is no difference between the analogs shown in Figs. 2 and 3a. Both can replicate the stress-strain data, if the model parameters are set as described above. Both satisfy the laws of thermodynamics (see Einav, 2004). The question is then: are they really equally relevant?

To question this, let us now consider a separate scenario: this time we get a 'real' material that is made from two randomly distributed elasto-plastic phases (as shown in Fig. 4a). Assume that in this material:

(1) the solid fractions of the distinct phases are ϕ_1 and ϕ_2,

(2) the corresponding stiffness of each of the two phases is h_1 and h_2; we set $E_i = h_i\phi_i$ for i = 1 or 2,

(3) the corresponding strength of each of the two phases is k_1 and k_2.

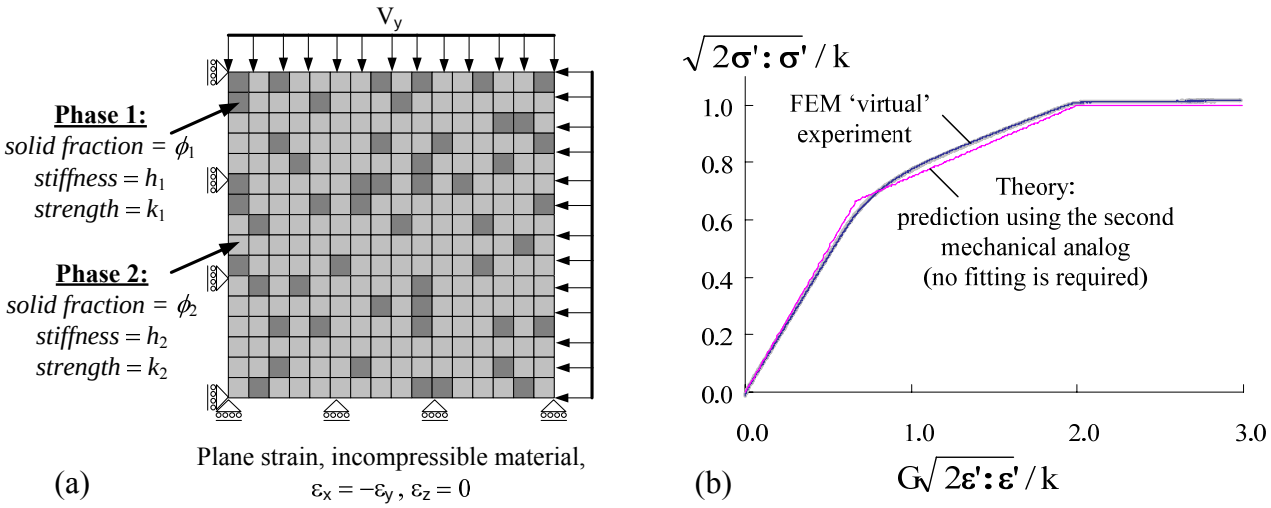

Figure 4. (a) a random two-phase elasto-plastic material, subjected to an isochoric plane shear test (asymptotically, as an infinitely large chessboard problem with infinitesimal sub-elements). (b) the shear stress-strain curve of the random material as extracted from a virtual FEM simulation; this experiment is predicted quite remarkably via the simple analog model of section 2.2, without applying any curve-fitting, but using the same physical parameters.

Now consider the particular case of a random two-phase elasto-plastic material whose second phase is infinitely strong ($k_2 \to \infty$). Obviously, if the local strains were found to be distributed uniformly across the real material sample, then its effective constitutive response would be that of the second analog, as shown in Fig. 1, with effective macroscopic properties that are given by eqs. (5), (8), and (9). The success of the second analog depends on the crudeness of the strain equivalence assumption. In random two-phase *elastic* material, the strain equivalence is known to provide an upper bound for the true overall stiffness (e.g., Doghri, 2000); in random two-phase *rigid perfectly plastic* material, this assumption provides an upper bound to the true overall collapse stress (e.g., Ostoja-Starzewski and Ilies, 1996).

Let us investigate the practicality of the strain-equivalence assumption in the more general case of a random elasto-plastic material (with all of the coefficients of stiffness and strength being finite), and evaluate the success of the simple analog of section 2.2 to predict experiments without curve-fitting. For that purpose consider the following virtual experiment. Take a two-phase random von-Mises elasto-plastic material, as shown in Fig. 4a. For a given solid fraction of the phases whose stiffness and strength are known, it is possible to compare the prediction of the analog (with its extension to 3D, viz. eq. (10)) against results from a virtual isochoric shear experiment using the finite element method (FEM). The simple analog predicts quite remarkably the experiment, as shown in Fig 4b. In our view, this demonstration should motivate to seriously consider aborting models that are based on the first analog of section 2.1., and start using the second alternative of section 2.2.

3. Generalisation of the micromechanical analog

3.1. A one-dimensional model for random elasto-plastic material

We extend the logic of the second analog (section 2.2) to that shown in Fig. 5a: the so-called Masing-Iwan model (Masing, 1926; Iwan, 1966). It is well established that this analog results in the typical stress-strain curve presented in Fig. 5b. Hysteresis response is still observable but the stress-strain curve is characterised by a gradually changing slope. This time we do not have a single yield mechanism, but rather have a continuous yielding. Again, by adopting the strain equivalence assumption, this analog can be interpreted for a general random elasto-plastic material, in terms of an infinite number of elasto-plastic phases, i.e., where the stiffness and strength coefficients follow a certain probability distribution. For simplicity, in the following we describe only two ideal cases: (1) a constant strength but variable stiffness, and (2) a constant stiffness by variable strength. In order to be consistent with our previous section we adopt a slightly different analysis from that of Einav and Collins (2008). While the concept is similar, it seems that the current analysis is more convenient.

Assume that the strength is constant across the material and equal k, and denote $\phi(\eta)$ as the solid fraction of all of the elements η with stiffness $h(\eta-d\eta/2)<h(\eta)<h(\eta+d\eta/2)$. We can write the following, simply by extending the corresponding equations in section 2.2:

$$E = \int \phi(\eta)h(\eta)d\eta \; ; \; k(\eta)=k \tag{12}$$

$$\int \phi(\eta)d\eta = 1 \tag{13}$$

$$y(\sigma_\eta,\eta) = \sigma_\eta(\eta)^2 - k^2 \le 0 \tag{14}$$

$$\sigma_\eta(\eta) = h(\eta)\varepsilon_e(\eta) \tag{15}$$

$$\varepsilon_e(\eta) = \varepsilon - \varepsilon_p(\eta) \tag{16}$$

$$\sigma = \int \phi(\eta)\sigma_\eta(\eta)d\eta = \int \phi(\eta)h(\eta)\varepsilon_e(\eta)d\eta = E\varepsilon - \int \phi(\eta)h(\eta)\varepsilon_p(\eta)d\eta \tag{17}$$

Eq. (12) shows that the average stiffness E is the statistical mean of the distributed phases' stiffness $h(\eta)$, where the solid fraction $\phi(\eta)$ plays the role of a probability density function, according to Eq. (13), in the spirit of homogenisation. Eq. (14) represents the yield criterion of element η, whose local stress is $\sigma_\eta(\eta)$. Eq. (15) denotes the local elastic law of that stress. Eq. (16) arises from compatibility, the decomposition of the total strains into elastic and plastic local strains, $\varepsilon_e(\eta)$ and $\varepsilon_p(\eta)$, and the assumption of strain equivalence $\varepsilon(\eta)=\varepsilon$ for any η. The last equation, eq. (17), represents equilibrium.

We can conceive that overall failure would occur when all of the slider elements yield, i.e., when the equality in (14) is met for any η. In that case the ultimate stress is given by $\sigma_u = \pm k$.

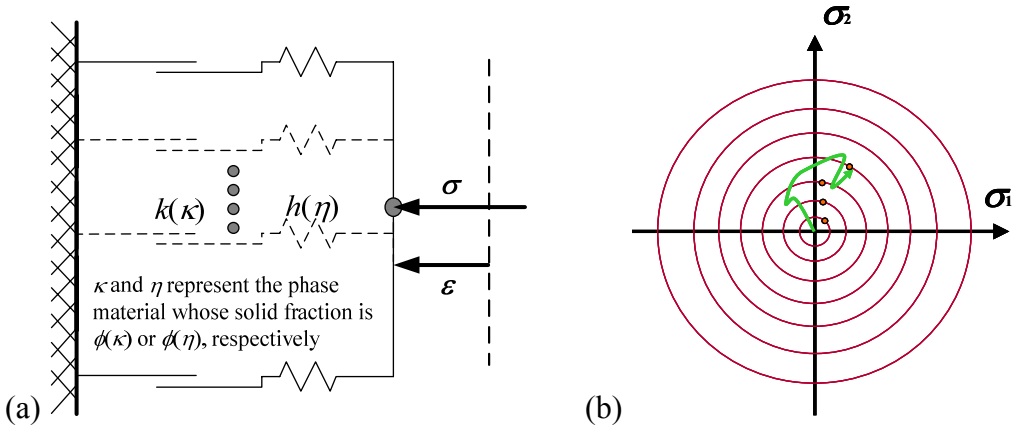

Figure 5. (a) a distributed parallel spring-slide analog. (b) an extension of the scalar model to account for the more general tensorial case is possible by replacing the 1D sliders using infinite number of yield surfaces (here via a 2D representation)

Now consider the case that the stiffness of all the elements is constant and equal E, and denote $\phi(\kappa)$ as the solid fraction of all of the elements κ with strength in the range $k(\kappa-d\kappa/2)<k(\kappa)<k(\kappa+d\kappa/2)$. We can write the following equations, replacing those in (12-17):

$$\sigma_u = \int \phi(\kappa)k(\kappa)d\kappa \,,\; h(\kappa)=E \tag{18}$$

$$\int \phi(\kappa)d\kappa = 1 \tag{19}$$

$$y(\sigma_\kappa,\kappa) = \sigma_\kappa(\kappa)^2 - k(\kappa)^2 \le 0 \tag{20}$$

$$\sigma_\kappa(\kappa) = E\varepsilon_e(\kappa) \tag{21}$$

$$\varepsilon_e(\kappa) = \varepsilon - \varepsilon_p(\kappa) \tag{22}$$

$$\sigma = \int \phi(\kappa)\sigma_\kappa(\kappa)d\kappa = E\int \phi(\kappa)\varepsilon_e(\kappa)d\kappa = E\left(\varepsilon - \int \phi(\kappa)\varepsilon_p(\kappa)d\kappa\right) \tag{23}$$

The conceptual result is similar to that of the variable stiffness model case in eqs. (12-17).

The tensorial form of the above model was proposed recently by Einav and Collins (2008), proving consistency with the first and second laws of thermodynamics. In the spirit of eqs. (10) and (11), it is sufficient for now to note that the major difference is attributed introducing associated flow rules to the local yield surfaces; these two properties (yield criterion and flow rule) are written as follows (e.g., for the constant strength case):

$$y_\kappa(\boldsymbol{\sigma}_\kappa,\kappa) = 2\boldsymbol{\sigma}'_\kappa(\kappa) : \boldsymbol{\sigma}'_\kappa(\kappa) - k(\kappa)^2 \le 0 \tag{24}$$

$$\delta\boldsymbol{\varepsilon}'_p(\kappa) = \lambda(\kappa)\partial y_\kappa(\boldsymbol{\sigma}_\kappa,\kappa)/\partial\boldsymbol{\sigma}'_\kappa(\kappa) = 2\lambda(\kappa)\boldsymbol{\sigma}'_\kappa(\kappa) \tag{25}$$

Therefore, the extension into the tensorial form entails that the sliders could be replaced by a series of nested and stationary yield surfaces (see Fig. 6a)

3.2. The micromechanical interpretation

In both studied cases (constant stiffness or strength), it can be confirmed that the two most important observable parameters, the overall stiffness E (here constant) and strength σ_u are practically predictable directly from micromechanical information of local parameters, again under the assumption that the strain is uniform across the sample. Whether we should make use of the

constant spring model, the constant strength model, or their combination (a possible extension) is not a question of phenomenology but a question of the material at hand. In many materials, the stiffness is fairly constant across the sample, while the strength is prone to vary quite significantly (for example, Weibullian strength of brittle particles (Weibull, 1951)). In that respect it is important to mention the contribution of Chaboche (2003) who presented a theory with some similarities to the above, although neglecting the random aspects of the property distributions, connection to phenomenological plasticity, and extensibility to tensorial models.

In accord with the tensorial model, we find that each of the yield surfaces bound a single 'micro' stress $\boldsymbol{\sigma}_{\kappa}(\kappa)$. Since the macro-stress is the average of the micro-stresses, the overall 'macro' behaviour of the macroscopic stress-strain curve should follow a gradually flattening curve during proportional loading thanks to the gradual yielding of the local stresses. For a Weibull distribution of strengths, the closed form solution of such a stress-strain curve was given by Einav and Collins (2008), based on the spring-slider analog. To demonstrate that this model provides an adequate representation of a general random multi-phase elasto-plastic material, albeit the strain equivalence assumption, a comparison of the theory against virtual FEM simulations (with Weibull statistic of strength) is presented in terms of the stress-strain curve during hysteresis loading. The corresponding strength contours are shown along with the boundary condition of isochoric shear in Fig. 6a, while the prediction of the analog model to the hysteresis cycle is demonstrated in Fig. 6b.

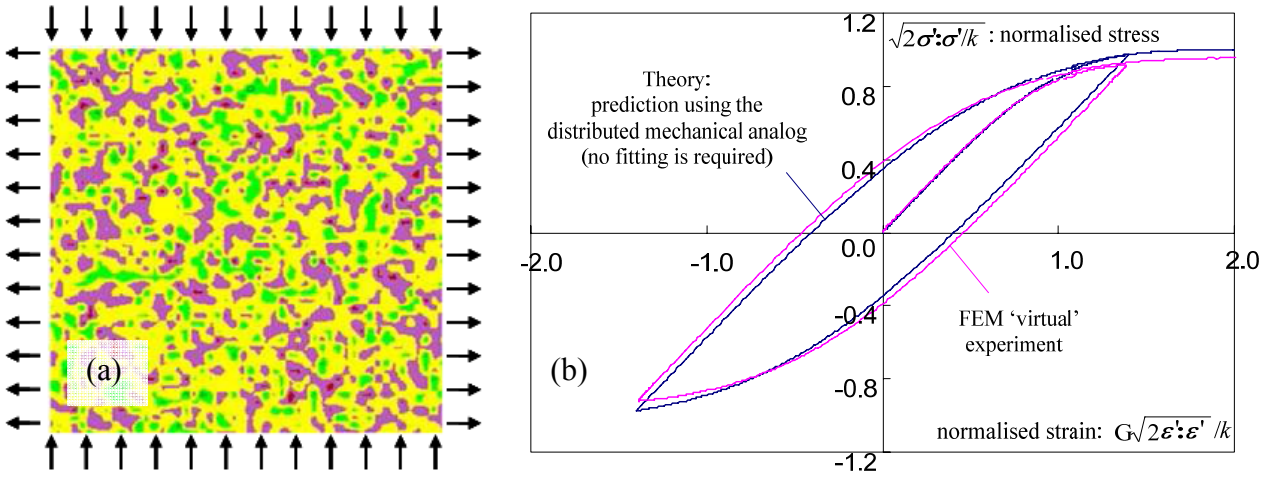

Figure 6. (a) a random multi-phase elasto-plastic material, subjected to an isochoric plane shear test (contours represent the strength coefficient); (b) the analog prediction to a virtual experiment of multi-phase random elasto-plastic material with variable strength using the FEM (as shown by the inset: taken from Einav & Collins, 2008). No fitting is required since the parameters of the FEM and analog are exactly the same.

3.3. Discussion about the physics of kinematic hardening

Recall the Iwan-Mroz analog model (Iwan, 1967; Mroz, 1967). In this model a single free spring is connected in a series to many individual 'parallel spring-slider elements', each of which is in a series with the next parallel spring-slider element in the line. While the stress is uniform along the various spring-slider elements (and the free spring), it is hard to see how this model could be interpreted for the currently studied random elasto-plastic material, even under an assumption of uniform stress. For example, it is hard to establish to which physical parameter the free spring of the Iwan-Mroz model could be connected. Nevertheless, this analog is commonly the starting point of kinematic hardening plasticity models. In the general tensorial case, each of the sliders is being replaced by a yield surface. All of these yield surfaces can translate in the space of sub-element stresses (here, the stress acting on a unit of parallel spring and slider) via the 'translation rule', representing the difference between the stresses within the springs and sliders of those sub-elements.

It seems that the popularity of this 'series' Iwan-Mroz model brought many researchers in the soil mechanics community to adopt the misconception that 'kinematic hardening' is the outcome of translating yield surfaces in stress-space. But this is a rather phenomenological description, and not a micromechanical interpretation; in the previous subsection, however, we did find a way to connect an analog to the physical properties, i.e., via the extension of the 'parallel' Masing–Iwan model. Einav (2004) discusses more about the differences between the thermodynamics potentials of the 'series' Iwan-Mroz and the 'parallel' Masing-Iwan model; it can be shown that the Iwan-Mroz model introduces an undesirable term to the Helmholtz free energy, that introduces the translation rules for the yield surfaces. Following Collins and Einav (2005) it can be supported that this assumption is only phenomenological, and arise directly from heterogeneities of local stresses across the sample. This is, however, being directly captured by the 'series' Masing-Iwan model. As motivated before and elaborated by Einav and Collins (2008), the internal variables of the 'parallel' Masing-Iwan model posses a clearer physical meaning, related to the statistics of yielding within a representative volume element. This is the reason for the presence of 'kinematic hardening' in terms of the observed hysteresis.

4. Isotropic hardening: phenomenology and micromechanical origins

In the traditional Critical State Soil Mechanics (CSSM, Roscoe & Schofield, 1963) approach the experimentally-fitted normal compression curve is applied to drive the modelled hardening process. This way of modelling neglects the underlying micromechanical processes that govern the hardening behaviour of the material, that most importantly differ between different geomaterials. As a consequence, it is difficult to determine the associated parameters that are used in CSSM without further experiments if the conditions vary. A typical constitutive assumption is frequently introduced by proposing that the yield surface grows isotropically (Fig. 7a) at a certain rate that is determined by a curve fitting hardening parameter λ either in terms of growing void ratio, plastic volumetric strain, or total volumetric strain. For example, the original expression for the pre-consolidation pressure in those models is given by (see schematic representation in Fig. 7b):

$$p_c = p_c(v) = p_r \exp\left(\frac{v_\lambda - v}{\lambda}\right) \tag{26}$$

where $v = 1+e$ is the specific volume (with e being the void ratio); p_r is a reference quantity with the dimensions of stress that is normally having the value 1kPa. In this model the void ratio is related to the logarithm of the pressure, by introducing the parameter, λ, the so-called normal consolidation compression modulus. This is an additional fitting parameter, which may not be necessary, as we later argue, if first principle of energy balance are considered adequately, at least when modelling brittle granular materials.

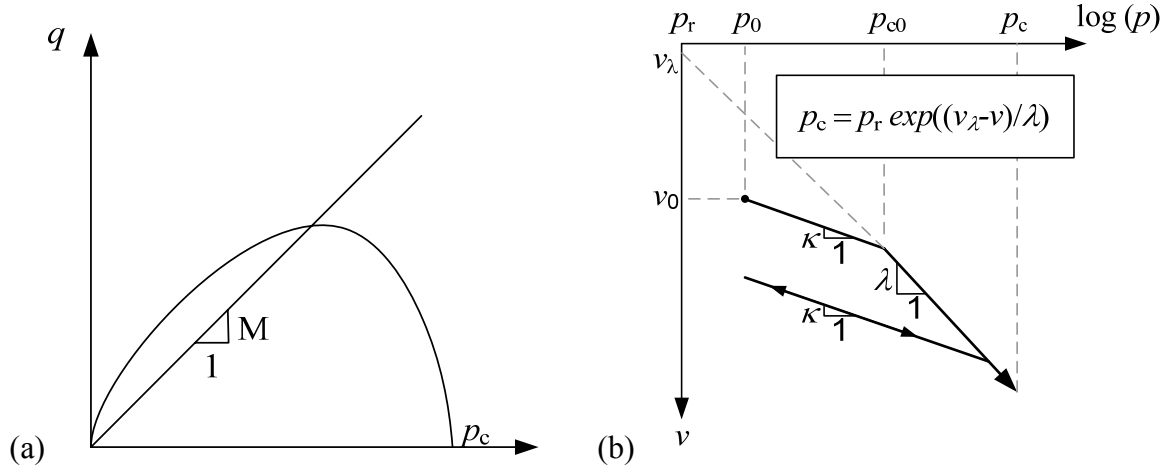

Figure 7. (a) typical yield surface in models of CSSM; (b) schematics of isotropic hardening, representing the growths of the yield surface's largest pressure p_c.

4.1. A brief review on breakage mechanics

Thus far we managed to provide an explanation to the micromechanics behind kinematic hardening, via the parallel Masing-Iwan model. In the previous subsection we have introduced the problem of observed isotropic hardening, and stated the common phenomenological model assumption in CSSM. In order to be able to explain isotropic hardening via first principles, it is necessary to employ a new theory, which we call Breakage Mechanics (Einav, 2007a & 2007b), along with the definition of a new internal (and measurable) variable, called 'breakage' *B*.

It is known that the shifting of the grain size distribution (gsd) due to comminution is the dominant governing mechanism of the isotropic hardening phenomenon observed on macroscopic scale in brittle granular materials. Therefore in micromechanics based constitutive modelling, this shifting gsd should be introduced to obtain the overall material behaviour. Einav (2007a) finds a way to express this requirement in a thermodynamically consistent way by relating the evolving gsd to the initial ($p_0(d)$) and ultimate ($p_u(d)$) ones via the internal variable of breakage *B*:

$$p(d) = p_0(d)(1-B) + p_u(d)B \tag{27}$$

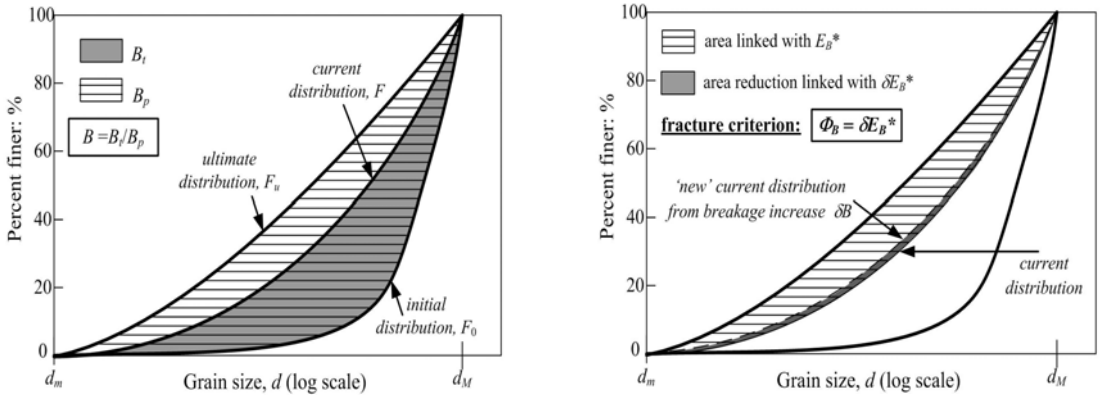

Figure 8. The breakage measurement and evolution law (Einav, 2007a,c). The left figure (a) portrays the measurable definition of breakage. The right diagram (b) presents the breakage propagation criterion for granular materials. Φ_B is the breakage dissipation, denoting the energy consumption from incremental increase of breakage. δE_B^* is the incremental reduction in the residual breakage energy.

This breakage *B* is measurable, given the corresponding gsd area definition in Fig. 8a. The current gsd $p(d)$, expressed in terms of Breakage (eq. (27)), is used for statistical homogenization. This is somewhat equivalent to the statistical averaging using the solid fraction $\phi(\eta)$ in section 3.1. However, while $\phi(\eta)$ is invariable in the previous definition, here the gsd $p(d)$ is evolving due to the crushing of the grains. The elastic strain energy of a volume element of granular material is given as the statistical average strain energy within all the grain size fractions within that volume:

$$\Psi = \int_{d_m}^{d_M} p(d)\psi(d,\boldsymbol{\varepsilon})\mathrm{d}d \tag{28}$$

where d_m and d_M are the minimum and maximum grain sizes, respectively. In this averaging process, the hypothesis of energy split (Einav, 2007a) is used, which suggests that the energy stored in a grain size fraction *d* is scaled by a non-dimensional factor $f(d) = (d/d_r)^n$:

$$\psi(d,\boldsymbol{\varepsilon}) = f(d)\psi_r(\boldsymbol{\varepsilon}) \tag{29}$$

In the above $d_r = <d^n>_0^{1/n}$ is being used as the reference grain size; *n* represents the dimension of the system; $\psi_r(\boldsymbol{\varepsilon})$ is expressed in term of the total strain tensor $\boldsymbol{\varepsilon}$ and represents the elastic strain energy in the reference grain d_r. The energy scaling in eq. (29) has been verified by DEM analysis

(Einav, 2007a). As a consequence of the energy split hypothesis, the Helmholtz energy potential is obtained in the form (Einav, 2007a):

$$\Psi = (1 - \vartheta B)\psi_r(\boldsymbol{\varepsilon}) \tag{30}$$

This expression, along with the equation of the proximity index property $\vartheta = 1 - < d^2 >_u / < d^2 >_0$, are the result of the same statistical homogenisation procedure. The proximity index property measures the "distance" between the initial and ultimate gsd's, with $< d^2 >_u$ and $< d^2 >_0$ being the second order moments of the ultimate and initial grain size distribution functions (by mass). From eq. (30), and consideration of thermodynamics, the energy conjugated to the breakage variable (the 'breakage energy') is defined as:

$$E_B = -\frac{\partial \Psi}{\partial B} = -\vartheta \psi_r(\boldsymbol{\varepsilon}) \tag{31}$$

The crushing of particles creates new surface areas which leads to energy release via the dissipation (termed Φ_B). It is then proposed that the breakage dissipation is driven by the loss of strain energy in the particles, as schematically portrayed in Fig. 8b and mathematically expressed by:

$$\Phi_B = \delta E_B^* \tag{32}$$

$$E_B^* = (1 - B)E_B \tag{33}$$

where E_B^*, the 'residual breakage energy', represents the available energy in the system for the crushing process (Einav, 2007a).

The yield criterion, which signifies the onset and then governs the evolution of breakage, can be worked out from (32) and (33) (Einav, 2007c):

$$y_B = (1 - B)^2 E_B - E_c = 0 \tag{34}$$

where E_c isthe critical breakage energy, a constant that arises directly from the derivation process. The introduction of the yield criterion requires the specification of the analysis to rate-independent processes, suggesting that during dissipation $E_B = \partial \Phi_B / \partial B$, and $\Phi_B = (\partial \Phi_B / \partial B)\delta B$.

4.2. General breakage models

We have briefly shown in the preceding section some of the fundamentals of Breakage Mechanics, based on first principles of energy balance and statistical homogenisation; this is a very convenient starting point for the formulation of micromechanics-based constitutive models of crushable granular materials. In this section we show how these principles could be applied to derive simple (and thermodynamically consistent) constitutive models. We also plan to highlight how the success of predicting the observed behaviour can be improved by considering the underlying elastic laws that govern the contact behaviour at the micro scales, not by adding more parameters.

The Helmholtz free energy potential Ψ and dissipation potential Φ, from which all other constitutive equations are derived, take the following general forms:

$$\Psi = (1 - \vartheta B)\left[\psi_v\left(\varepsilon_v^e\right) + \psi_s\left(\varepsilon_v^e, \varepsilon_s^e\right)\right] \tag{35}$$

$$\Phi = \sqrt{{\Phi_B}^2 + {\Phi_p^v}^2 + {\Phi_p^s}^2} \tag{36}$$

in which standard notations in soil mechanics are used: p and q denote mean effective stress and shear stress; ε_v^e and ε_s^e are elastic volumetric strain and shear strain, respectively. Functions ψ_v and ψ_s in (35) govern the elastic volumetric and shear behaviours of the model, and represent the

'unbroken' stored energy in a reference particle size d_r. The dissipation potential Φ comprises three parts corresponding to breakage dissipation Φ_B, plastic volumetric dissipation Φ_p^v and plastic shear dissipation Φ_p^s (Nguyen and Einav, 2009):

$$\Phi_B = \frac{\sqrt{2E_B E_c}}{(1-B)}\delta B \tag{37}$$

$$\Phi_p^v = \frac{p}{(1-B)}\sqrt{\frac{2E_c}{E_B}}\delta\varepsilon_v^p \tag{38}$$

$$\Phi_p^s = Mp\left|\delta\varepsilon_s^p\right| \tag{39}$$

In the above equations $M = q_u / p_u$ is the ratio between the ultimate shear stress q_u and ultimate volumetric stress p_u at failure (i.e., related to the ultimate mobilised friction angle); ε_v^p and ε_s^p are the plastic volumetric strain and shear strain, respectively. The constitutive relationships can be obtained from the free energy potential as follows:

$$p = \frac{\partial\Psi}{\partial\varepsilon_v^e} = (1-\vartheta B)\left(\frac{\partial\psi_v}{\partial\varepsilon_v^e} + \frac{\partial\psi_s}{\partial\varepsilon_v^e}\right) \tag{40}$$

$$q = \frac{\partial\Psi}{\partial\varepsilon_s^e} = (1-\vartheta B)\frac{\partial\psi_s}{\partial\varepsilon_s^e} \tag{41}$$

$$E_B = -\frac{\partial\Psi}{\partial B} = \vartheta\left[\psi_v\left(\varepsilon_v^e\right) + \psi_s\left(\varepsilon_v^e, \varepsilon_s^e\right)\right] \tag{42}$$

The yield function y^* in dissipative stress space is obtained as a result of the degenerate Legendre transformation of the dissipation potential (36) (see further details in Nguyen and Einav, 2009). Using (37-39), y^* can be replaced by the mixed breakage/yield function:

$$y_{\text{mix}} = \frac{E_B(1-B)^2}{E_c} + \left(\frac{q}{Mp}\right)^2 - 1 \le 0 \tag{43}$$

and the following flow rules applies ($\delta\lambda$ is a common non-negative multiplier): $\delta B = \delta\lambda.\partial y^* / \partial E_B$, $\delta\varepsilon_v^p = \delta\lambda.\partial y^* / \partial p$, $\delta\varepsilon_s^p = \delta\lambda.\partial y^* / \partial q$. All of this is the outcome of careful consideration of thermodynamics (Nguyen and Einav, 2009). Examination of the yield criterion (43) highlights that the breakage energy E_B drives the isotropic hardening process and allows capturing this process in a natural way, without having to introduce any *ad hoc* parameters. The hardening of the material during comminution is directly driven by the competition between E_B and $(1–B)^2$: as B grows towards unity, E_B must increase to balance the equality in eq. (34). Since E_B is a function of the elastic stored energy, and governs the rate of dissipation during the crushing process, any improvement in the elastic behaviour of the model will automatically result in improvements in post yield behaviour. We believe that this aspect is a genuine step ahead, which allows us to be more economic in introducing model parameters, all by applying first principles.

The best example is our capability to eliminate parameters such as the normally-consolidated compression modulus λ in CSSM (see eq. (26) and Fig. 7b), which bears no direct physical meaning but is purely being a fitting parameter. This economy in model parameters is discussed at

length in Einav (2007d), highlighting that the modelling of crushable granular materials using CSSM should require at least four additional ad-hoc parameters to achieve the same level of detail.

In the following we demonstrate how change in the elasticity law carries out changes to the post-yielding hardening behaviour. Nguyen and Einav (2009) further demonstrate the success of these changes in predicting experimental results.

4.3. Isotropic hardening via breakage model based on linear contact law

Linear elasticity is the simplest elastic law possible, which requires two constant parameters, e.g., the bulk and shear modulii K and G. For this purpose, ψ_v and ψ_s are defined as follows:

$$\psi_v = \frac{1}{2} K \varepsilon_v^{e\,2} \tag{44}$$

$$\psi_s = \frac{3}{2} G \varepsilon_s^{e\,2} \tag{45}$$

In this case, the breakage/yield surface (43) is rewritten in true triaxial stress space as:

$$y = \frac{\vartheta}{2E_c}\left(\frac{1-B}{1-\vartheta B}\right)^2\left(\frac{p^2}{K}+\frac{q^2}{3G}\right)+\left(\frac{q}{Mp}\right)^2 - 1 \le 0 \tag{46}$$

Fig. 9a shows the complete picture of the breakage/yield surface and its evolution in triaxial stress space.

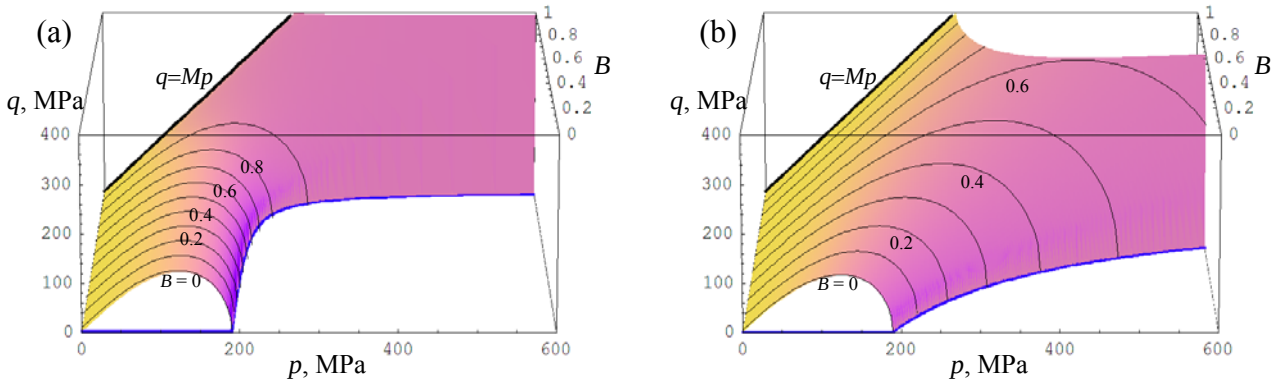

Figure 9: Yield/breakage surface in *p*-*q*-*B* space, using: (a) linear elastic contact law (Einav, 2007d), and (b) Hertzian- like contact law (Nguyen and Einav, 2009).

Solving eq. (46) for $q = 0$ and $B = 0$, the initial crushing pressure p_{c0} in isotropic compression is given by:

$$p_{c0} = \sqrt{\frac{2KE_c}{\vartheta}} \tag{47}$$

As discussed by Einav (2000c), this relation bears striking relation to Griffith's (1921) criterion in fracture mechanics. As the breakage grows, we predict isotropic hardening of the yield pressure in terms of the breakage:

$$p_c = \left(\frac{1-\vartheta B}{1-B}\right) p_{c0} \tag{48}$$

since ϑ is between zero and one. This simple model was motivated by Einav (2007d) as a "student model" to illustrate some features of breakage mechanics models. In the next section we further advance the model, slightly increasing the complexity, but not the number of parameters.

4.4. Isotropic hardening via breakage model based on non-linear contact law

Enhancement to the model response can be made by developing appropriate nonlinear (hyper)elastic terms ψ_v and ψ_s, to account for pressure-dependent bulk and shear modulii. The following forms of ψ_v and ψ_s were derived for this purpose (Einav, 2007b; Nguyen and Einav, 2009):

$$\psi_v = p_r \frac{\left[\xi\left(\varepsilon_v^e\right)/p_r\right]^{2-m}}{\overline{K}(2-m)} \tag{49}$$

$$\psi_s = \frac{3}{2} p_r \overline{G} \left[\frac{\xi\left(\varepsilon_v^e\right)}{p_r}\right]^m \varepsilon_s^{e\,2} \tag{50}$$

where $\xi\left(\varepsilon_v^e\right) = p_r \sqrt[1-m]{\overline{K}(1-m)\left(\varepsilon_v^e - \varepsilon_{vr}\right)+1}$ and p_r is defined as a reference pressure conveniently taken as 1 kPa; $m = \frac{1}{3}$ for Hertzian contact, or $m = \frac{1}{2}$ as per classical finding in soil mechanics, $\overline{K}$ and $\overline{G}$ are non-dimensional material constants, which replace the dimensional K and G in linear elastic contact model, and ε_{vr} the initial volumetric strain dependent on the maximum $e_{\max}$ and initial e_0 void ratios of the sample (Einav, 2007d): $\varepsilon_{vr} = -\log\left((1+e_0)/(1+e_{\max})\right)$.

The breakage criterion can be written in triaxial stress space as:

$$y = \frac{\vartheta(1-B)^2}{E_c}\left[\frac{p_r A^{\frac{2-m}{1-m}}}{\overline{K}(2-m)} + \frac{q^2 A^{\frac{-m}{1-m}}}{6(1-\vartheta B)^2 p_r \overline{G}}\right] + \left(\frac{q}{Mp}\right)^2 - 1 \le 0 \tag{51}$$

where

$$A = \left(\frac{3p\overline{G} + \sqrt{9p^2\overline{G}^2 - 6\overline{G}m\overline{K}q^2}}{6(1-\vartheta B)p_r\overline{G}}\right)^{1-m} \tag{52}$$

In this case, the crushing pressure p_{c0} in isotropic compression becomes:

$$p_{c0} = p_r\left[\frac{(2-m)\overline{K}E_c}{\vartheta p_r}\right]^{\frac{1}{2-m}} \tag{53}$$

As breakage evolves, we predict isotropic hardening of the yield pressure in terms of the breakage:

$$p_c = \frac{(1-\vartheta B)}{(1-B)^{2/(2-m)}} p_{c0} \tag{54}$$

Comparing eq. (54) and (48), it is clear that the elasticity law changes the isotropic hardening post yielding. The effects of this on the shape of the entire yield/breakage surface ($q \neq 0$) can be seen in Fig. 9. In particular, note the difference in the evolution of the surface's largest pressure with increasing breakage when the non-linear elasticity is applied (Fig. 9b) compared to the case of linear isotropic elasticity (Fig. 9a). Nguyen and Einav (2009) demonstrate the success of this consideration in improving predictions, without adding fitting parameters. Of particular interest are comparisons against the experiments by Wong *et al.* (1997), and thereafter the discussion concerning the energy balance during cataclastic shear.

5. Conclusions

We have illustrated the importance and the advantages of micromechanics-based constitutive models for geomaterials with particular attentions to issues related with isotropic and kinematic hardening. These phenomena are usually described by classical phenomenological models of plasticity at continuum scale, without resorting to the micro-structural changes at lower scales. Unlike phenomenological models, which require the introduction of *ad hoc* fitting parameters, micromechanics-based models have the advantage of facilitating explicit links between model parameters and the underlying microstructural properties. Moreover, the number of parameters can be kept minimal for even greater capability in model predictions.

In relation to kinematic hardening, we looked at two distinct spring-slider analog systems. We have argued that the use of the parallel spring-slider model is advantageous, compared to the series spring-slider model since it enables to describe random elasto-plastic media without introducing unphysical parameters. In relation to isotropic hardening, we looked at models based on the Breakage Mechanics theory. Thanks to the explicit links between the macroscopic model behaviour and the physics of grain crushing, the improvements of model predictions at macro scale can be achieved simply by enhancing the contact law at grain scale. No further parameters are required in this process.

6. Acknowledgments

Itai Einav would like to acknowledge the Australian Research Council's for the *Discovery Projects* funding scheme (project number DP0774006). Giang Nguyen wishes to thank the University of Sydney for the financial support through the University of Sydney Postdoctoral Fellowship and the Bridging Support Grant.

7. References

Chaboche J.L. 2003. Thermodynamics of local state: overall aspects and micromechanics based constitutive relations. pp. 113–129 in Technische Mechanik, Manuskripteingang, 11. Juni 2003. Band 23, Heft 2-4.

Collins I.F., Einav I. 2005. On the validity of elastic/plastic decompositions in soil mechanics. *Proceeding of Symposium on Elastoplasticity*. Kyushu University, Japan, T. Tanaka and T. Okayasu (eds), 193-200.

Cundall P.A., Strack O.D.L. 1979. A discrete numerical model for granular assemblies. Geotechnique 29(1), 47-65.

Doghri I. 2000. Mechanics of deformable solids. Linear, nonlinear, analytical and computational aspects, Springer, Berlin.

Einav I., 2004. Thermomechanical relations between basic stress-space and strain-space models. Géotechnique. Vol. 54(5). pp., 315-318.

Einav I., 2007a. Breakage mechanics--Part I: Theory, Journal of the mechanics and physics of solids 55(6), 1274-1297.

Einav I., 2007b. Breakage mechanics--Part II: Modelling granular materials, Journal of the mechanics and physics of solids 55(6), 1298-1320.

Einav I., 2007c. Fracture propagation in brittle granular matter, Proceedings of the Royal Society A: Mathematical, Physical and Engineering Sciences 463(2087), 3021-3035.

Einav I. 2007d. Soil mechanics: breaking ground, Philosophical Transactions of the Royal Society A: Mathematical, Physical and Engineering Sciences 365(1861), 2985-3002

Einav I., Collins I.F. 2008. A thermo-mechanical framework of plasticity based on probabilistic micro-mechanics. Journal of Mechanics of Materials and Structures, 3(5), 867-92.

Griffith A.A. 1921. The Phenomena of Rupture and Flow in Solids, Philosophical Transactions of the Royal Society of London. Series A, Containing Papers of a Math. or Phys. Character (1896-1934) 221(-1), 163-198.

Iwan W.D. 1966. A distributed element model for hysteresis and its steady-state dynamic response. J. App. Mech. Trans. ASME, 33(4), 893-900.

Iwan W.D. 1967. On a class of models for the yielding behaviour of continuous and composite systems. J. App. Mech., 34, 612-617.

Masing G. 1926. Eigenspannungen und verfestigung beim messing. Proc. 2nd Int. Congr. App. Mech.

Maugin G.A. 1992. The thermomechanics of plasticity and fracture. Cambridge University Press.

Mroz Z. 1967. On the description of anisotropic work hardening. J. Mech. Phys. Solids, 15, 163-175.

Nguyen G.D., Einav I., 2009. Cataclasis and permeability reduction: an energetic approach based on breakage mechanics, Pure and applied geophysics, 166 (2009) 1–32.

Schofield A.N., Wroth C.P. 1968. Critical state soil mechanics. London: McGraw-Hill.

Ostoja-Starzewski M., Ilies H. 1996. The Cauchy and characteristic boundary value problems of random rigid-perfectly plastic media. International Journal of Solids and Structures. 33(8), 1119-1136.

Weibull W. 1951. A statistical distribution function of wide applicability. J. Appl. Mech. (Trans. ASME) 18, 293–297.

Wong T., David C. and Zhu W. 1997. The transition from brittle faulting to cataclastic flow in porous sandstones: Mechanical deformation. Journal of Geophysical Research 102(B2)**,** 3009-3025.